Anomalous ion transport in saline solutions under electric fields: A molecular dynamic study

Marie Landeiro dos Reis, S. Touzain, A. El Hamidi

Anomalous ion transport in saline solutions under electric fields : A molecular dynamic study

M. Landeiro Dos Reis, S. Touzain, and A. El Hamidi
LaSIE UMR CNRS 7356, La Rochelle Université,
Av. Michel Crépeau, 17042, La Rochelle Cedex 1, France *
(Dated: January 15, 2026)

In this study, we employ molecular dynamics simulations to investigate the anomalous diffusion of Na^+ and Cl^- ions in water at the microscopic scale. By carefully distinguishing the migration (drift) component from the diffusive motion, we analyze the influence of ion concentration and applied electric fields on ionic transport. Our results reveal clear deviations from classical Brownian dynamics under non-zero electric fields, highlighting the emergence of anomalous diffusion regimes. We further show that the degree of anomalous behavior strongly depends on the ionic chemical activity and the strength of Coulombic interactions between ions.

I. INTRODUCTION

Classical diffusion models are based on the assumption that diffusing particles follow Brownian motion. This theoretical framework implies a linear growth of the mean squared displacement (MSD), $\langle r^2(t)\rangle \propto t$, as established by the foundational works of Louis Bachelier [1] and Albert Einstein in 1905 [2].

While this framework successfully describes diffusion in several systems, both experimental and theoretical studies have highlighted deviations from this linear behavior in complex environments such as biological media, porous materials, or systems under external fields [3–5]. These situations are referred to as anomalous diffusion, characterized by a fractional power-law scaling of the form $\langle r^\beta(t)\rangle \propto Dt^\alpha$, where the exponents $\alpha \neq 1$ and $\beta \neq 2$ indicate non-classical transport behaviors, and D denotes a generalized diffusion coefficient. The nonlinearity may arise from time dependence ($\alpha \neq 1$) [3, 4, 6–10] or spatial dependence ($\beta \neq 2$) [4, 11, 12].

In this work, we investigate the ionic diffusion of saline solutions under the influence of an external electric field. A thorough understanding of this phenomenon is crucial for advancing electrochemical water desalination technologies [13–16], which are increasingly recognized for their energy efficiency and environmental sustainability [17]. Beyond desalination, electric-field-driven ionic transport plays a key role in biological and biochemical applications, such as electrophoresis used to separate charged biomolecules like proteins, DNA, and RNA [18] and in the study of ion mobility within biological environments, including cell membranes and tissues [19].

Several experimental studies, notably in electrochemical impedance, have revealed that ionic diffusion can deviate from this classical model, particularly in confined environments or under electric fields, and exhibit anomalous diffusion of the form $\langle r^2(t)\rangle \propto t^\alpha$ with $\alpha \neq 1$ [3, 10, 20, 21].

To investigate ionic transport phenomena, several modeling approaches are available, each with its own strengths and limitations: (i) The Poisson-Nernst-Planck (PNP) model [22–26] employs a mean-field approach by iteratively solving the Poisson and Nernst-Planck equations. Ion flow is represented as a continuous concentration profile, driven by electrostatic potential force and ion concentration gradient. Although computationally efficient, it approximates critical effects, such as the finite size of the ions and discrete charges. (ii) Brownian dynamics (BD) [24, 25, 27] explicitly simulating the motion of mobile ions while treating the surrounding water implicitly as a continuum. The motion of ions is governed by the Langevin equation, which incorporates forces such as frictional and random forces from the solvent and electrostatic interactions with other ions, calculated by solving the Poisson equation. (iii) Hybrid methods that combine the Poisson-Nernst-Planck (PNP) model with Monte Carlo simulations [28] or dynamic lattice Monte Carlo [29] have been developed to improve the description of ions that are treated explicitly. These approaches enhance the accuracy of ion transport modeling by incorporating molecular-level ion interactions within a continuum framework. (iv) Atomistic calculations, such as molecular dynamics (MD) simulations [30–35], provide a complete framework to study ion transport by explicitly modeling atomic-level interactions.

Despite growing interest, the microscopic origin of anomalous ion transport under external fields remains poorly understood. In this study, we employ molecular dynamics simulations combined with a anomalous diffusion framework to investigate the transport properties of Na^+ and Cl^- ions in saline solutions. By extracting the anomalous diffusion exponent α, we aim to quantify deviations from classical diffusion and to explore how these deviations depend on ion concentration and the strength of an externally applied electric field. This atomistic perspective provides new insights into the mechanisms driving anomalous transport in confined or driven ionic systems.

* Contact author: mlandeir@univ-lr.fr

II. METHODOLOGY

Molecular dynamics simulations were conducted using the Large-scale Atomic/Molecular Massively Parallel Simulator (LAMMPS) [36]. The atomic visualization were performed using OVITO [37]. The simulation cell consists of two electrodes with a saline solution placed between them. Periodic boundary conditions were applied in the x and y directions, while there was free surface in the z direction (see Fig. 1). The system contain N particles, comprising n_{H_2O} water molecules, n_{Cl^-} chloride ions and n_{Na^+} sodium ions. All parameters for the size of the simulation cell is given Tab. I. The electrodes were modeled as a body-centered cubic conductive metal (M) (Tab. II), aimed solely to generate an electric field within the saltwater solution. To immobilize the electrodes, forces on all atoms in the electrodes were set to zero, effectively freezing their positions. We ensured that the system size was sufficient to accurately address diffusion-related phenomena [38].

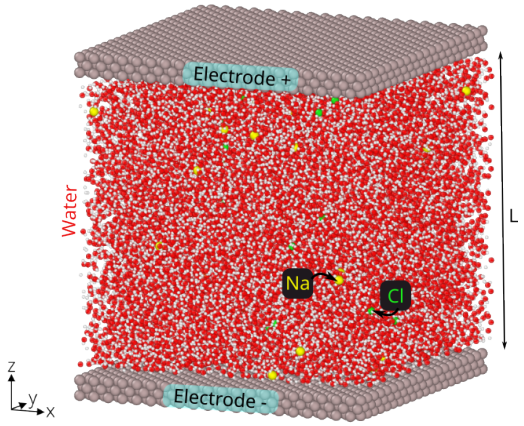

FIG. 1. Simulation cell.

TABLE I. Simulation cell parameters. The inter-electrode distance is denoted as L, while d_x, d_y, and d_z represent the cell dimensions in the x, y, and z directions (Fig. 1). The number of water molecules is noted as n_{H_2O}, and n_M refers to the number of atoms in the electrodes.

L (Å)	d_x (Å)	d_y (Å)	d_z (Å)	n_{H_2O}	n_M
90	79	79	95	≃18200	4800

The interatomic potential used is a combination of Coulombic interactions and a simple Lennard-Jones (LJ) potential. The potential energy, for the particule i writes:

$$V(\mathbf{r_i}) = \underbrace{\sum_{j\neq i} \frac{q_i q_j e^2}{r_{ij}}}_{\text{Coulomb}} + \underbrace{\sum_{j\neq i} 4\varepsilon_{ij}\left[\left(\frac{\sigma_{ij}}{r_{ij}}\right)^{12} - \left(\frac{\sigma_{ij}}{r_{ij}}\right)^{6}\right]}_{\text{LJ}} \tag{1}$$

where $\mathbf{r_i}$ is the position of the particle i, q_i is the charge of the particle i, e is the elementary charge, r_{ij} is the distance between the particles i and j, ε_{ij} and σ_{ij} are respectively the potential depth and the distance parameter of the LJ contribution.

The parameters of the potential $V(\mathbf{r_i})$ (Eq. 1) are provided in Table II. A rigid water model based on TIP4P/2005 [39] was used, while the parameters for Na^+ and Cl^- ions were derived from the CHARMM-27 force field [40]. The long-range Coulombic interactions were accounted for using the FFT-based particle-particle/particle-mesh (PPPM) method in LAMMPS [36].

TABLE II. LJ pair potential parameters used in this study [39, 40].

	σ_{ij} (Å)	ε_{ij} (kcal/mol)
O-O	0.185199	3.1589
Na-Na	0.04690	2.4299
Cl-Cl	0.1500	4.04470
M-M	11.697	2.574
O - M	0.4	2.86645

System equilibration was achieved through a 1 ns NVE simulation at 300 K, *i.e* in the microcanonical ensemble, ensuring energy stabilization and convergence of the interelectrode distance. Following equilibration, a 1 ns NVT simulation was performed to study the diffusion of water, *i.e* in the canonical ensemble, with or without charge of the electrodes. For the NVT simulations we used a Nose Hoover thermostat. Hence, the equations of motion are those given by of Shinoda *et al* [41], combining the hydrostatic equations of Martyna *et al* [42] with the strain energy of Parrinello and Rahman [43]. The time integration schemes are based on Verlet [44].

We investigated the influence of ion concentration and electrode charge on ionic diffusion. To ensure robust statistical sampling, 50 molecular dynamics simulations were conducted for each combination of concentration (ranging from 4 g/L to 36 g/L of NaCl solution) and charge of the atoms within the electrode, quoted q^M. The charge q^M was varied from $0e$ to $0.05e$ per metallic atom on the cathode and from $0e$ to $-0.05e$ on the anode, corresponding to average electric field strengths between approximately 1×10^5 V/m ($q^M \approx 0.001e$) and 1×10^7 V/m ($q^M \approx 0.05e$).

III. RESULTS

To characterize the diffusion processes at play, we directly extracted from our MD simulations the Mean Squared Displacement (MSD) for each type of ion without (Fig. 2(a)) and with electric field (Fig. 2(b)-(c)), using:

$$< \mathbf{r}^2_{ion}(t) >= \frac{1}{N_{ion}} \sum_{i=1}^{N_{ion}} \|\mathbf{r_i}(t) - \mathbf{r_i}(0)\|^2 \tag{2}$$

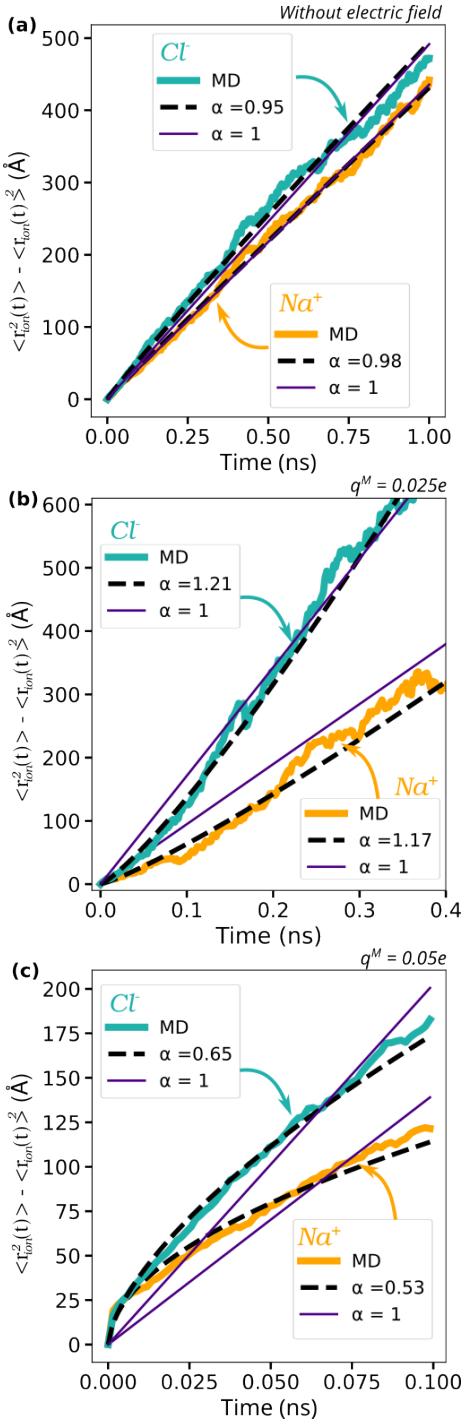

FIG. 2. Comparison between $\langle \mathbf{r}_{ion}^2(t)\rangle - \langle \mathbf{r}_{ion}(t)\rangle^2$ obtained from molecular dynamics simulations and the predictions of Eq. 3. **(a)** Without external electric field at an ion concentration of 36 g/L. **(b)** Under an external electric field with $q^M = 0.025e$ of 5 g/L. **(c)** Under an external electric field with $q^M = 0.05e$ and an ion concentration of 36 g/L. In each case, the dashed black line corresponds to normal diffusion ($\alpha = 1$), while the purple line represents the best fit obtained by treating α as a free parameter.

where N_{ion} represents the number of ions in the solution and $\|\mathbf{r_i}(t) - \mathbf{r_i}(0)\|$ is the distance traveled by ion i, between instants 0, the beginning of the NVT simulation procedure, and t. The distinct behavior of Na^+ and Cl^- ions will be carefully analyzed in Eq. 2.

To extract the diffusion coefficient and assess whether the diffusion is anomalous, we compared the MSD from MD simulations (Eq. 2) with the following diffusion model, where the MSD of mobile ions is described by a fractional time dependence:

$$< \mathbf{r}_{ion}^2(t) > - < \mathbf{r}_{ion}(t) >^2 = \frac{6D_{ion}}{\Gamma(1+\alpha)} t^{\alpha} \qquad (3)$$

where D_{ion} is the diffusion coefficient, $0 < \alpha \leq 2$ is a real number characterising the subdiffusion ($\alpha < 1$) or surdiffusion ($\alpha > 1$) process. $\Gamma(1+\alpha)$ is the gamma function, an extension of the factorial function for complex and real numbers. One note that in case of normal diffusion, $\alpha = 1$ and $\Gamma(1+\alpha) = 1$. The adjustable parameters in this model are α, D_{ion}. The term $< \mathbf{r}_{ion}(t) >^2$ accounts for the systematic drift of the charged particle under an external field, and must be considered to isolate the purely diffusive contribution to the mean square displacement. In such a case, the particle acquires a net average velocity, commonly referred to as the drift velocity, denoted by $\mathbf{v}_d$:

$$\mathbf{v}_d = \frac{d}{dt} < \mathbf{r}_{ion}(t) > = \frac{\beta \mathbf{v}}{\Gamma(1+\beta)} t^{\beta-1} \qquad (4)$$

where $\mathbf{v} = (v_x, v_y, v_z)$ is a constant and β a fractional coefficient that can be different from α.

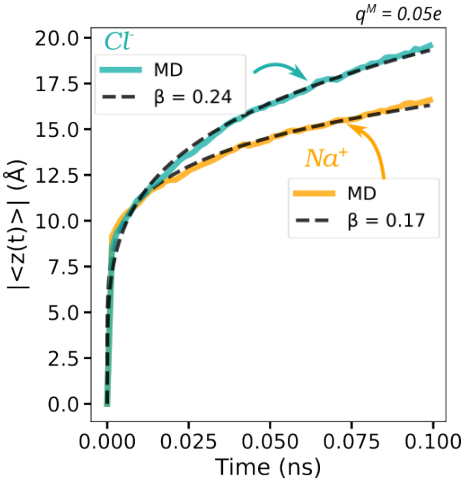

FIG. 3. Comparison of $| < z(t) > |$ obtained with MD simulations with the predictions of Eq. 6 under elastic field with $q^M = 0.05e$. The ion concentration is 36g/L.

In this context, the flux $\mathbf{J}$ of the n ions, which quantifies the net transport of ions, can be expressed as:

$$\mathbf{J} = n\mathbf{v}_d. \qquad (5)$$

In our case, the electric field is applied only along z, thus $\mathbf{J} = (0, 0, J)$. By fitting the mean ion displacement from MD simulations to the anomalous drift expression

$$< \mathbf{r}_{ion}(t) >= \frac{\mathbf{v}t^{\beta}}{\Gamma(1+\beta)} \tag{6}$$

we extracted the anomalous drift exponent β and the drift velocity $\mathbf{v} = (0, 0, v)$ (Fig. 3). Since the applied electric field is oriented along the z-axis, the mean displacement can be written as $< z(t) >= \frac{vt^{\beta}}{\Gamma(1+\beta)}$ where $z(t)$ represents the ion drift along the z-direction.

For each simulation, to confirm the relevance of a anomalous model, we compared Eq. 3 with fitted α and D_{ion} (see black dashed lines Fig. 2 to Eq. 3 with α fixed at 1 (see purple lines on Fig. 2), corresponding to a normal diffusion model.

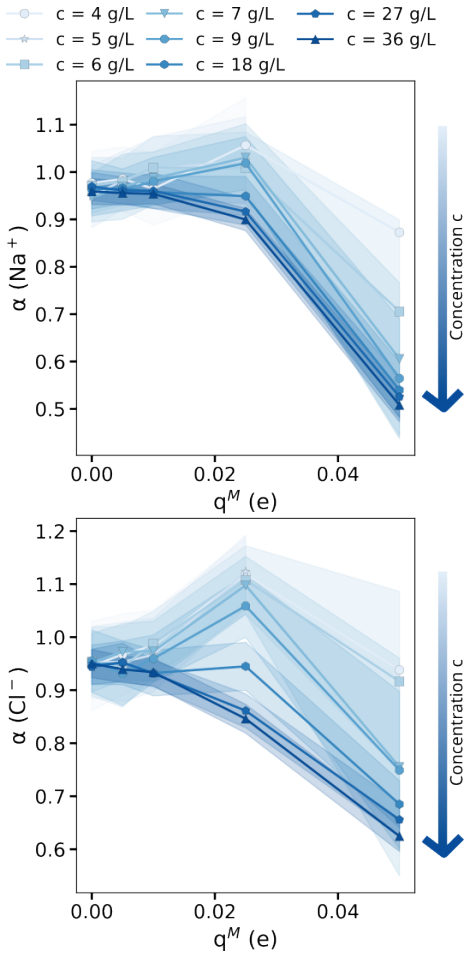

FIG. 4. Mean value of the fractional coefficient α from Eq. 3 as a function of the charge q^M of metallic atoms composing the electrodes. The standard deviation is shown as a transparent overlay.

We plot Fig. 3 an example of simulation without electric field for a ionic concentration of 36g/L. In the absence of an applied electric field (i.e., uncharged electrodes, $q^M = 0e$), our results show that a classical diffusion model accurately describes the ion dynamics (see Fig. 3). In this regime, both Na^+ and Cl^- ions exhibit quasi-Brownian motion, characterized by a diffusion exponent $\alpha \simeq 1$. Although their diffusion behaviors are qualitatively similar, the slopes of their mean squared displacements differ, reflecting different diffusion coefficients. We obtain D_{Na^+} between 0.7 and 0.9x10^{-9}m^2/s and D_{Cl^-} between 0.8 and 1.1x10^{-9} m^2/s. These values are consistent with those reported in the literature that found around 1x10^{-9} m^2/s for D_{Na^+} and arround 2x10^{-9} m^2/s for D_{Cl^-} [45–48]. Note that this diffusion coefficient is highly temperature-dependent. In this work, the temperature is fixed at 300K. A study at different temperatures will be carried out in future work.

We plot Fig. 2(b)-(c) some examples of simulations under electric field, respectivelely with $q^M = 0.025e$ and $q^M = 0.05e$, for a concentration of 9g/L and 36g/L. When the system is subjected to an electric field, the mean squared displacement (MSD) exhibits a nonlinear time dependence, indicating anomalous diffusion characterized by $\alpha \neq 1$ in Eq. 3. In this case, the transport of ions becomes biased, forcing negatively charged ions to migrate towards the positive electrode and vice versa. We can note that the behavior of the MSD over time follows the same trend regardless of the ions.

It is interesting to note that the type of anomalous diffusion depends on the electric field. Indeed, at low fields, the diffusion is slightly accelerated ($\alpha > 1$), whereas at high fields, the diffusion is slowed down ($\alpha < 1$). However, it is important to note that at high fields, the simulation times are very short (0.1 ns), and very quickly all ions become fixed on the electrodes (see Fig. 2(c)).

In order to obtain reliable statistics for the value of α as a function of ion type, concentration, and electrode charge q^M, we averaged the results from 50 simulations for each set of parameters. The results are shown Fig. 4. The standard deviation is displayed as a shaded region to illustrate the statistical uncertainty associated with the estimation of α. We plot the variation of α as a function of the charge q^M, and thus the electric field, for the different concentrations tested.

The behavior of α is complex and highly dependent on concentration (Fig. 4). At low concentrations, a superdiffusion phenomenon is observed, which increases with the electric field ($\alpha > 1$). Regardless of the concentration studied, as previously shown we then find that, this effect reverses at high electric fields, where the ions quickly reach the electrode surfaces.

For electrode charges below $0.025e$, Fig. 4 shows that the degree of anomalous diffusion decreases as the ion concentration increases. Indeed, α approaches 1 for concentrations above 18 g/L, indicating a diffusion behavior increasingly close to the classical Brownian regime.

The same tendency can be anticipated from Fig. 5, which presents the evolution of the diffusion coefficient D_{ion} as a function of the applied charge q^M for the different concentrations studied. It can be hypothesized that, at low concentrations, diffusion might be boosted by the

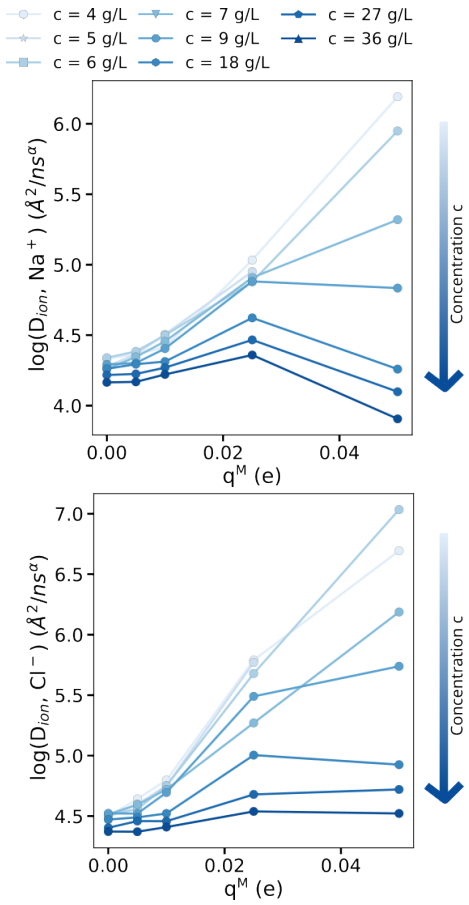

FIG. 5. Mean value of the fractional coefficient D_{ion} from Eq. 3 as a function of the charge q^M of metallic atoms composing the electrodes.

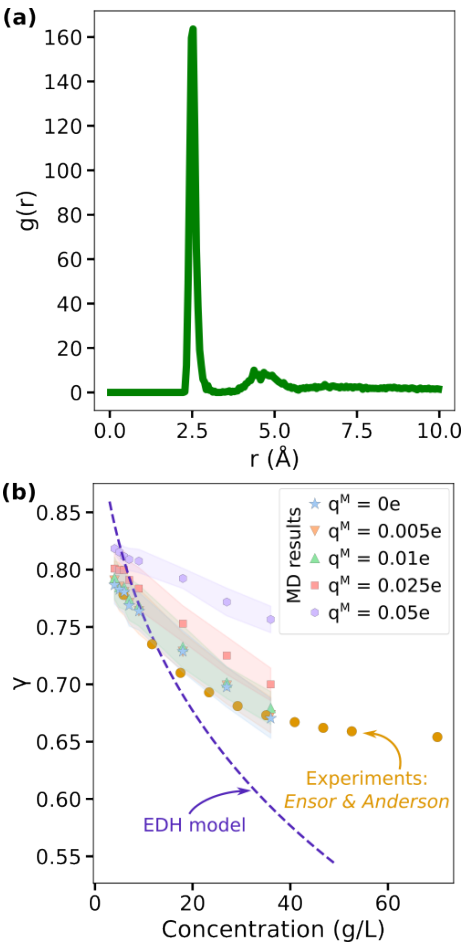

FIG. 6. (a) Na^+-Cl^- pair correlation function $g(r)$ as function of the distance from the center of the particle r at c= 27 g/L. (b) Comparison of the activity coefficient γ deduced from our MD results compared to the Extended Debye-Hückel (EDH) model [49] (Eq. 8) and experiments of Ensor and Anderson [50].

electric field due to enhanced ionic mobility. However, this effect could progressively vanish at higher concentrations, where ion–ion interactions and crowding effects are expected to play a dominant role. Above 18 g/L, the influence of q^M on D_{ion} may therefore become negligible.

At higher concentrations, it is possible that electrostatic interactions between oppositely charged ions lead to the formation of ionic pairs such as Na^+/Cl^-. These paired entities, being closer to electrically neutral, may respond less strongly to the applied electric field, since the net force acting on them could be reduced. As a result, their contribution to directed ion transport might be limited, which could appear as a decrease in the effective diffusion coefficient.

To gain a better understanding of this phenomenon, which appears to be linked to the increasing Coulombic interactions between ions at higher concentrations, we examined the average number of Na^+/Cl^- ion pairs, denoted as N_{pairs}, as a function of ion concentration and charge q^M. A pair is considered to be formed when the distance between a Na^+ and a Cl^- ion is less than a_i = 2.5Å, based on the first peak of the radial distribution function (RDF) obtained from our molecular dynamics simulations (Fig. 6(a)). Note that the value of a_i found is in agreement with the experimental value of 2.35Å[49]. We then estimated an effective activity coefficient γ, being roughly the ratio of free (unpaired) ions to the total number of ions in solution:

$$\gamma \propto \frac{N_{ion} - N_{pairs}}{N_{ion}} \tag{7}$$

We harshly adjust the coefficient of proportionality to 0.82 to fit the experimental results of Ensor and Anderson [50] obtained without applied electric field (Fig. 6(b)). Then we confront our results to the Extend Debye Hückel (EDH) model [49]:

$$-\log_{10}\gamma = \frac{A_m |q_{Na^+} q_{Cl^-}| I_m^{1/2}}{1 + B_m a_i I_m^{1/2}} \tag{8}$$

with A_m and B_m two coefficient and I_m the ionic strengh:

$$A_m = \left(\frac{2\pi N_a}{1000}\right)^{1/2} \times \frac{e^3}{2.3026(k_B T \epsilon_r)^{3/2}} \tag{9}$$

,

$$B_m = \left(\frac{8\pi N_a}{1000}\right)^{1/2} \times \frac{e}{(k_B T \epsilon_r)^{1/2}} \tag{10}$$

and

$$I_m = \frac{1}{2}\frac{c}{m_{NaCl}}\left(v_{Na^+} + v_{Cl^-}\right) \tag{11}$$

where $m_{NaCl} = 58.44$g/mol is the molar mass of NaCl, q_{Na^+} and q_{Cl^-} are respectively the charge of Na^+ and Cl^-, v_{Na^+} and v_{Cl^-} are respectively the valance of Na^+ and Cl^-, N_a is the Avogadro constant, k_B the Boltzmann constant and $\epsilon_r = 65$ is the dielectric permittivity constant [51].

We plot the results Fig. 6(b). As commonly observed, the EDH model (Eq. 8) tends to underestimate the activity coefficient γ at high concentrations. This limitation arises because the model cannot fully capture the complexity of ion–ion interactions, particularly salt effects and short-range correlations [49, 51].

In agreement with experiments, we show that the activity coefficient γ decreases significantly with increasing ion concentration, reaching a value of approximately 0.7 at 36 g/L (see Fig. 6(b)). This behavior can be attributed to the sharp increase in the number of ion pairs formed at higher concentrations: as the average distance between ions decreases, the likelihood of forming pairs between oppositely charged species (Na^+ and Cl^-) increases. When such ion pairs form, they can be considered quasi neutral over long distances. As a result, the electric field has a reduced effect on these neutral entities. This could explain why the deviation of α from 1 indicative of anomalous diffusion tends to diminish as the ion concentration increases.

Moreover, the results show that the stronger the applied electric field (i.e., for larger values of q^M), the higher the activity coefficient γ. This is because the electric field tends to counteract the attractive Coulomb interactions between oppositely charged ions. If the force induced by the electric field is strong enough, it can break apart the formed ion pairs, thereby increasing the number of free ions in solution and raising the value of γ.

In Fig. 7, we present the evolution of the fractional drift exponent β, extracted from Eq. 6 and used in the calculation of the ionic flux (Eq. 5). The results consistently show that $\beta < \alpha$, indicating that the collective ionic transport, the drift, is more hindered than individual diffusion. This difference suggests that while ions undergo subdiffusive motion, their macroscopic drift under an applied field exhibits an even stronger deviation from normal transport dynamics.

Furthermore, one note that as the applied charge q^M increases, β departs further from 1 and appears to converge toward a limiting value. This trend may reflect a

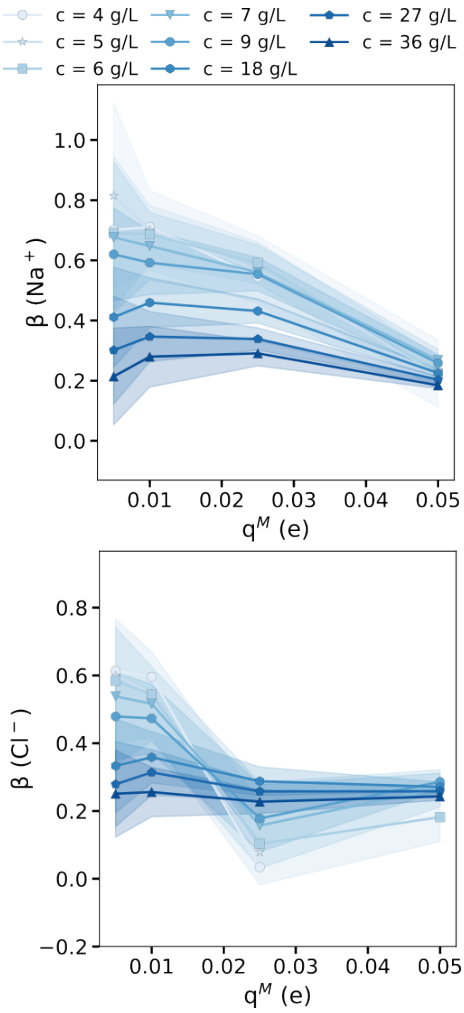

FIG. 7. Mean value of the fractional coefficient β from Eq. 6 as a function of the charge q^M of the metallic atoms composing the electrodes. The standard deviation is shown as a transparent overlay.

transition from a weak-field regime, where ion motion remains partially Brownian, to a strong-field regime dominated by correlated and constrained dynamics. Under high electric fields, ion–ion interactions and local structuring effects (as illustrated in Fig. 6) become increasingly significant, imposing collective constraints that limit the system's ability to respond linearly to the external forcing.

Furthermore, the drift velocity v, shown in Fig. 8, increases markedly with the applied charge q^M. This trend reflects both an enhanced driving force under higher fields and a nonlinear response of the ionic system, suggesting that the electric field not only accelerates ion motion but also amplifies the underlying anomalous transport behavior.

It is interesting to note that we were able to decouple the contribution of migration (drift) from that of diffusion. Our results indicate that migration exhibits a more pronounced anomalous behavior than diffusion, suggest-

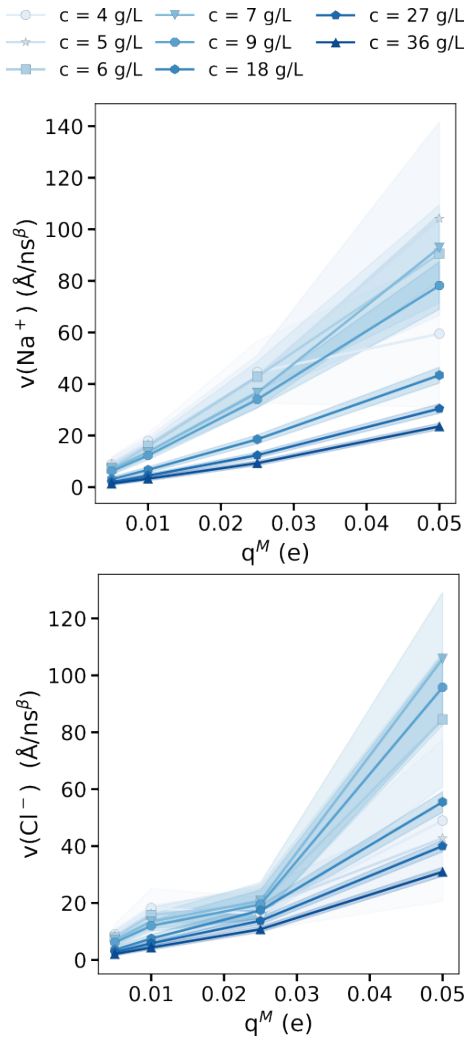

FIG. 8. Mean value of the drift velocity v from Eq. 6 as a function of the charge q^M of the metallic atoms composing the electrodes. The standard deviation is shown as a transparent overlay.

ing that the collective transport of ions under an electric field is more strongly influenced by constraints and correlations than individual diffusive motion.

Bridging atomistic molecular dynamics with continuum or mesoscopic models remains an important but nontrivial task. From MD simulations, several microscopic quantities such as the diffusion coefficient, the anomalous exponents α (for diffusion) and β (for drift), and the steady-state ionic flux (Eq. 5) can be extracted and used to parameterize or validate higher-scale transport models. These quantities provide direct physical input for generalized frameworks such as fractional Poisson–Nernst–Planck equations or memory-dependent Langevin formulations, where anomalous transport is described through non-local temporal kernels or distributed mobility [22–26]. However, establishing a rigorous correspondence between these atomistic observables and macroscopic transport coefficients requires systematic coarse-graining and averaging over time and space, which represents a significant research effort that we plan to undertake in future work.

IV. CONCLUSION

In this work, we investigated the diffusion dynamics of ionic species in aqueous saline solution under the influence of an external electric field, using molecular dynamics simulations. By analyzing the mean squared displacement (MSD) of ions, we highlight that the transport process cannot always be accurately captured by a classical Brownian model. This is in agreement with impedance measurements and previous analyses [20, 21]. In particular, we found that the presence of an electric field induces anomalous diffusion, characterized by a nonlinear time dependence of the MSD and quantified by a fractional exponent $\alpha \neq 1$.

Our analysis revealed that, in the absence of an electric field, ion dynamics closely follow normal diffusion behavior, characterized by a diffusion exponent $\alpha \approx 1$. Moreover, the diffusion coefficients extracted from our simulations are in good agreement with experimental values reported in the literature [45–48]. However, when an electric field is applied, the diffusion behavior becomes strongly dependent on both the strength field and ion concentration. At low concentrations and moderate electric field, we observed superdiffusive behavior ($\alpha > 1$), whereas at high field intensities, the dynamics became subdiffusive ($\alpha < 1$), likely due to rapid adsorption of ions onto the electrode surfaces.

Furthermore, we showed that ion concentration plays a critical role in modulating the diffusion regime. At high concentrations, ion–ion coulombic interactions promote the formation of quasi-neutral Na^+/Cl^- pairs, which reduce the effectiveness of the electric field in driving ion transport. This results in a lower diffusion coefficient and a diffusion regime closer to normal behavior, with α approaching 1. Our results thus reveal a delicate interplay between Coulomb interactions, electric field-driven migration, and ion pairing, which governs the nature of ion transport across different regimes.

Importantly, we demonstrated that assuming normal diffusion in regimes where $\alpha \neq 1$ can lead to a significant overestimation of the diffusion coefficient, especially at high electric strengths. This finding highlights the necessity of incorporating anomalous diffusion models when analyzing ion transport in such systems.

Beyond diffusion, we also quantified the anomalous drift behavior of ions under an external electric field. By fitting the mean displacement to a fractional drift law, we extracted the drift exponent β and the drift velocity v, which together determine the ionic flux $J = nv_d$. Interestingly, we found that β farthest from 1 than α, indicating that the collective migration of ions under an electric field is more hindered than their individual diffusion. This suggests that correlations and local struc-

turing effects play a dominant role in governing the overall transport dynamics, particularly under strong electric fields.

This work opens the door to future investigations aiming to bridge the gap between atomistic and macroscopic descriptions. Comparing the results of our molecular dynamics simulations with continuum models such as the Poisson–Nernst–Planck framework possibly extended to include anomalous dynamics could provide a more complete understanding of ion transport across scales. Such a multiscale approach is essential for the accurate modeling of electrochemical systems, energy storage devices, and biological ion channels. Finally, it is challenging to determine the exact origin of anomalous diffusion. This behavior may arise from the system's non-ergodicity, induced by the non-periodic boundary conditions (surface) in one direction, leading to a continuous system evolution as ions progressively attach to the electrodes. We will aim to address these questions in our future work.

ACKNOWLEDGMENTS

We warmly thank Dr Malo Duportal for the very fruitful discussions we had, which significantly helped improve this work. The computational resources utilized for this study were graciously provided by the MCIA (Mésocentre de Calcul Intensif Aquitain) and the NOETHER computing facilities at La Rochelle University, hosted at the LaSIE laboratory and administered by Dr Antoine Falaize, to whom we are particularly grateful.

[1] L. Bachelier, Theory of speculation in the random character of stock market prices, MIT Press, Cambridge, Mass. Blattberg **1018**, 17 (1900).
[2] A. Einstein *et al.*, On the motion of small particles suspended in liquids at rest required by the molecular-kinetic theory of heat, Annalen der physik **17**, 208 (1905).
[3] R. Metzler, J.-H. Jeon, A. G. Cherstvy, and E. Barkai, Anomalous diffusion models and their properties: non-stationarity, non-ergodicity, and ageing at the centenary of single particle tracking, Physical Chemistry Chemical Physics **16**, 24128 (2014).
[4] P. Castiglione, A. Mazzino, P. Muratore-Ginanneschi, and A. Vulpiani, On *strong* anomalous diffusion, Physica D: Nonlinear Phenomena **134**, 75 (1999).
[5] D. Krapf, Chapter Five - Mechanisms Underlying Anomalous Diffusion in the Plasma Membrane, in *Current Topics in Membranes*, Lipid Domains, Vol. 75, edited by A. K. Kenworthy (Academic Press, 2015) pp. 167–207.
[6] P. Brault, C. Josserand, J.-M. Bauchire, A. Caillard, C. Charles, and R. W. Boswell, Anomalous Diffusion Mediated by Atom Deposition into a Porous Substrate, Physical Review Letters **102**, 045901 (2009).
[7] Y. Caspi, D. Zbaida, H. Cohen, and M. Elbaum, Anomalous Diffusion of High Molecular Weight Polyisopropylacrylamide in Nanopores, Macromolecules **42**, 760 (2009).
[8] C. D. Ball, N. D. MacWilliam, J. K. Percus, and R. K. Bowles, Normal and anomalous diffusion in highly confined hard disk fluid mixtures, The Journal of Chemical Physics **130**, 054504 (2009).
[9] M. Burgis, V. Schaller, M. Glässl, B. Kaiser, W. Köhler, A. Krekhov, and W. Zimmermann, Anomalous diffusion in viscosity landscapes, New Journal of Physics **13**, 043031 (2011).
[10] E. K. Lenzi, P. R. G. Fernandes, T. Petrucci, H. Mukai, H. V. Ribeiro, M. K. Lenzi, and G. Gonçalves, Anomalous Diffusion and Electrical Response of Ionic Solutions, International Journal of Electrochemical Science **8**, 2849 (2013).
[11] Y. Sagi, M. Brook, I. Almog, and N. Davidson, Observation of Anomalous Diffusion and Fractional Self-Similarity in One Dimension, Physical Review Letters **108**, 093002 (2012).
[12] B. O'Shaughnessy and I. Procaccia, Analytical Solutions for Diffusion on Fractal Objects, Physical Review Letters **54**, 455 (1985).
[13] M. Elimelech and W. A. Phillip, The Future of Seawater Desalination: Energy, Technology, and the Environment, Science **333**, 712 (2011).
[14] V. Bartzis and I. E. Sarris, A theoretical model for salt ion drift due to electric field suitable to seawater desalination, Desalination **473**, 114163 (2020).
[15] J. Azamat, Functionalized Graphene Nanosheet as a Membrane for Water Desalination Using Applied Electric Fields: Insights from Molecular Dynamics Simulations, The Journal of Physical Chemistry C **120**, 23883 (2016).
[16] M. Pasta, C. D. Wessells, Y. Cui, and F. La Mantia, A Desalination Battery, Nano Letters **12**, 839 (2012).
[17] J. Ahn, J. Lee, S. Kim, C. Kim, J. Lee, P. M. Biesheuvel, and J. Yoon, High performance electrochemical saline water desalination using silver and silver-chloride electrodes, Desalination **476**, 114216 (2020).
[18] J. R. Brody and S. E. Kern, History and principles of conductive media for standard dna electrophoresis, Analytical biochemistry **333**, 1 (2004).
[19] H. H. Ussing, Transport of ions across cellular membranes, Physiological reviews **29**, 127 (1949).
[20] E. K. Lenzi, P. R. G. Fernandes, T. Petrucci, H. Mukai, and H. V. Ribeiro, Anomalous-diffusion approach applied to the electrical response of water, Physical Review E **84**, 041128 (2011).
[21] E. K. Lenzi, H. V. Ribeiro, R. S. Zola, and L. R. Evangelista, Fractional Calculus in Electrical Impedance Spectroscopy: Poisson – Nernst – Planck model and Extensions, International Journal of Electrochemical Science **12**, 11677 (2017).
[22] R. Cherif, A. E. A. Hamami, A. Aït-Mokhtar, and W. Bosschaerts, Thermodynamic equilibria-based modelling of reactive chloride transport in blended cementitious materials, Cement and Concrete Research **156**, 106770 (2022).
[23] M. Rossi, T. Wallmersperger, S. Neukamm, and

K. Padberg-Gehle, Modeling and Simulation of Electrochemical Cells under Applied Voltage, Electrochimica Acta **258**, 241 (2017).

[24] B. Corry, S. Kuyucak, and S.-H. Chung, Tests of Continuum Theories as Models of Ion Channels. II. Poisson–Nernst–Planck Theory versus Brownian Dynamics, Biophysical Journal **78**, 2364 (2000).

[25] Q. Zheng and G.-W. Wei, Poisson–Boltzmann–Nernst–Planck model, The Journal of Chemical Physics **134**, 194101 (2011).

[26] D. Chen, Fractional Poisson–Nernst–Planck Model for Ion Channels I: Basic Formulations and Algorithms, Bulletin of Mathematical Biology **79**, 2696 (2017).

[27] C. Berti, S. Furini, D. Gillespie, D. Boda, R. S. Eisenberg, E. Sangiorgi, and C. Fiegna, Three-Dimensional Brownian Dynamics Simulator for the Study of Ion Permeation through Membrane Pores, Journal of Chemical Theory and Computation **10**, 2911 (2014).

[28] D. Boda and D. Gillespie, Steady-State Electrodiffusion from the Nernst–Planck Equation Coupled to Local Equilibrium Monte Carlo Simulations, Journal of Chemical Theory and Computation **8**, 824 (2012).

[29] P. Graf, A. Nitzan, M. G. Kurnikova, and R. D. Coalson, A Dynamic Lattice Monte Carlo Model of Ion Transport in Inhomogeneous Dielectric Environments: Method and Implementation, The Journal of Physical Chemistry B **104**, 12324 (2000).

[30] H. G. Hertz, A. V. J. Edge, and R. Mills, Velocity correlations in aqueous electrolyte solutions from diffusion, conductance and transference data. Application to concentrated solutions of cadmium iodide, Journal of the Chemical Society, Faraday Transactions 1: Physical Chemistry in Condensed Phases **79**, 1317 (1983).

[31] S. H. Lee and J. C. Rasaiah, Molecular dynamics simulation of ionic mobility. I. Alkali metal cations in water at 25°C, The Journal of Chemical Physics **101**, 6964 (1994).

[32] S. Chowdhuri and A. Chandra, Molecular dynamics simulations of aqueous NaCl and KCl solutions: Effects of ion concentration on the single-particle, pair, and collective dynamical properties of ions and water molecules, The Journal of Chemical Physics **115**, 3732 (2001).

[33] F. Sofos, T. E. Karakasidis, and D. Spetsiotis, Molecular dynamics simulations of ion separation in nano-channel water flows using an electric field, Molecular Simulation **45**, 1395 (2019).

[34] N. V. S. Avula, M. L. Klein, and S. Balasubramanian, Understanding the Anomalous Diffusion of Water in Aqueous Electrolytes Using Machine Learned Potentials, The Journal of Physical Chemistry Letters **14**, 9500 (2023).

[35] Y. Ding, A. A. Hassanali, and M. Parrinello, Anomalous water diffusion in salt solutions, Proceedings of the National Academy of Sciences **111**, 3310 (2014).

[36] A. P. Thompson, H. M. Aktulga, R. Berger, D. S. Bolintineanu, W. M. Brown, P. S. Crozier, P. J. in 't Veld, A. Kohlmeyer, S. G. Moore, T. D. Nguyen, R. Shan, M. J. Stevens, J. Tranchida, C. Trott, and S. J. Plimpton, LAMMPS - a flexible simulation tool for particle-based materials modeling at the atomic, meso, and continuum scales, Computer Physics Communications **271**, 108171 (2022).

[37] A. Stukowski, Visualization and analysis of atomistic simulation data with OVITO–the Open Visualization Tool, Modelling and Simulation in Materials Science and Engineering **18**, 015012 (2009).

[38] I. N. Tsimpanogiannis, O. A. Moultos, L. F. M. Franco, M. B. d. M. Spera, M. Erdős, and I. G. Economou, Self-diffusion coefficient of bulk and confined water: a critical review of classical molecular simulation studies, Molecular Simulation **45**, 425 (2019).

[39] J. L. F. Abascal, E. Sanz, R. García Fernández, and C. Vega, A potential model for the study of ices and amorphous water: TIP4P/Ice, The Journal of Chemical Physics **122**, 234511 (2005).

[40] A. D. MacKerell Jr., N. Banavali, and N. Foloppe, Development and current status of the CHARMM force field for nucleic acids, Biopolymers **56**, 257 (2000).

[41] W. Shinoda, M. Shiga, and M. Mikami, Rapid estimation of elastic constants by molecular dynamics simulation under constant stress, Physical Review B **69**, 134103 (2004).

[42] G. J. Martyna, D. J. Tobias, and M. L. Klein, Constant pressure molecular dynamics algorithms, J. chem. Phys **101**, 10 (1994).

[43] M. Parrinello and A. Rahman, Polymorphic transitions in single crystals: A new molecular dynamics method, Journal of Applied physics **52**, 7182 (1981).

[44] M. E. Tuckerman, J. Alejandre, R. López-Rendón, A. L. Jochim, and G. J. Martyna, A liouville-operator derived measure-preserving integrator for molecular dynamics simulations in the isothermal–isobaric ensemble, Journal of Physics A: Mathematical and General **39**, 5629 (2006).

[45] R. Mills, A Remeasurement of the Self-diffusion Coefficients of Sodium Ion in Aqueous Sodium Chloride Solutions, Journal of the American Chemical Society **77**, 6116 (1955).

[46] R. Mills, The Self-diffusion of Chloride Ion in Aqueous Alkali Chloride Solutions at 25°, The Journal of Physical Chemistry **61**, 1631 (1957), publisher: American Chemical Society.

[47] J. H. Wang, C. V. Robinson, and I. S. Edelman, Self-diffusion and Structure of Liquid Water. III. Measurement of the Self-diffusion of Liquid Water with H2, H3 and O18 as Tracers1, Journal of the American Chemical Society **75**, 466 (1953), publisher: American Chemical Society.

[48] P. Passiniemi, Accurate tracer diffusion coefficients of Na+ and Cl- ions in dilute aqueous sodium chloride solutions measured with the closed capillary method, Journal of Solution Chemistry **12**, 801 (1983).

[49] P. Rice, Handbook of aqueous electrolyte solutions: by al horvath; published by ellis horwood ltd., chichester, 1985; 211 pp. (1988).

[50] D. D. Ensor and H. L. Anderson, Heats of dilution of sodium chloride. temperature dependence, Journal of Chemical and Engineering Data **18**, 205 (1973).

[51] Z. Mester and A. Z. Panagiotopoulos, Mean ionic activity coefficients in aqueous nacl solutions from molecular dynamics simulations, The Journal of chemical physics **142** (2015).

[52] D. Gerasimov, The Nernst–Einstein equation for an anomalous diffusion at short spatial scales, Physica D: Nonlinear Phenomena **419**, 132851 (2021).